

**UCC Library and UCC researchers have made this item openly available.
Please [let us know](#) how this has helped you. Thanks!**

Title	Hot-electron injection in Au nanorod-ZnO nanowire hybrid device for near-infrared photodetection
Author(s)	Pescaglini, Andrea; Martín, Alfonso; Cammi, Davide; Juska, Gediminas; Ronning, Carsten; Pelucchi, Emanuele; Iacopino, Daniela
Publication date	2014-10-14
Original citation	Pescaglini, A., Martín, A., Cammi, D., Juska, G., Ronning, C., Pelucchi, E. and Iacopino, D. (2014) 'Hot-Electron Injection in Au Nanorod-ZnO Nanowire Hybrid Device for Near-Infrared Photodetection', Nano Letters, 14(11), pp. 6202-6209.
Type of publication	Article (peer-reviewed)
Link to publisher's version	https://pubs.acs.org/doi/abs/10.1021/nl5024854 http://dx.doi.org/10.1021/nl5024854 Access to the full text of the published version may require a subscription.
Rights	© 2014 American Chemical Society. This document is the Accepted Manuscript version of a Published Work that appeared in final form in Nano Letters, copyright © American Chemical Society after peer review and technical editing by the publisher. To access the final edited and published work see https://pubs.acs.org/doi/abs/10.1021/nl5024854
Item downloaded from	http://hdl.handle.net/10468/8136

Downloaded on 2023-03-23T07:22:59Z

Hot-Electron Injection in Au Nanorod-ZnO Nanowire Hybrid Device for Near-Infrared Photodetection

Andrea Pescaglino,[†] Alfonso Martín,[†] Davide Cammi,[‡] Gediminas Juska,[†] Carsten Ronning[‡]

Emanuele Pelucchi[†] and Daniela Iacopino^{†}*

Supporting information

Methods

ZnO nanostructures were grown by a simple vapor transport technique enabled by the vapor-liquid-solid (VLS) mechanism in a tube furnace at 1050 °C and 100 mbar, as reported elsewhere¹. Dimensional statistical analysis on the obtained nanowires, gave lengths between 1 μm to 10 μm with a mean value of 5 μm and diameters between 40 nm and 500 nm.

Gold nanorods were synthesized using a seed-mediated method described by El Sayed *et al.*² The as-prepared Au nanorod solution (1 mL) was centrifuged twice to remove hexadecyltrimethylammonium bromide (CTAB) excess and re-dispersed in 1 mL of deionized water with a resistivity of about 18 MΩ·cm. The final CTAB concentration was estimated to be 0.05 mM. It should be noticed that CTAB molecules form an organic double layer around Au nanorod metallic core that stabilizes nanorods in solution. The CTAB double layer has been estimated to be around 2.2 nm in thickness.³ Dimensional statistical analysis of 100 Au nanorods gave a mean nanorod length and diameter of 54 ± 3 nm and 22 ± 3 nm (aspect ratio of 2.4 ± 0.2),

respectively. Scanning electron microscopy (SEM) characterization was performed using a Scanning Electron Microscope (JSM 7500F, JEOL UK) at operating voltages of 10 kV.

Photoconductive measurements were carried out by mounting the sample on a home-made holder equipped with wire bonding to establish external electrical connections. Devices were kept in dark condition for at least a couple of hours until a steady dark-current value was reached. Wavefunction generator (SRS-DS360) was used to force a sinusoidal signal with amplitude 400 mV (frequency 19 Hz). The output signal was sent to a pre-amplifier (SRS-SR570) and the current measured with a SRS-SR830 lock-in amplifier using an acquisition time of 15 ms and an integration time of 10 ms. Devices were investigated at room temperature and illuminated using an UV portable lamp at 265nm and nominal power of 4 W (estimated intensity on the sample surface was 0.8 W/cm^2), and tunable supercontinuum source - a high-power Fianium fiber laser with an integrated acusto-optical filter operating in a pulsed-mode at 40 MHz with radiation wavelength tuning range of 600-1100 nm. The tunable laser was focused to a $\sim 2 \mu\text{m}$ diameter spot by using a 50x optical objective.

Electrical characterization of ZnO nanowire FET device

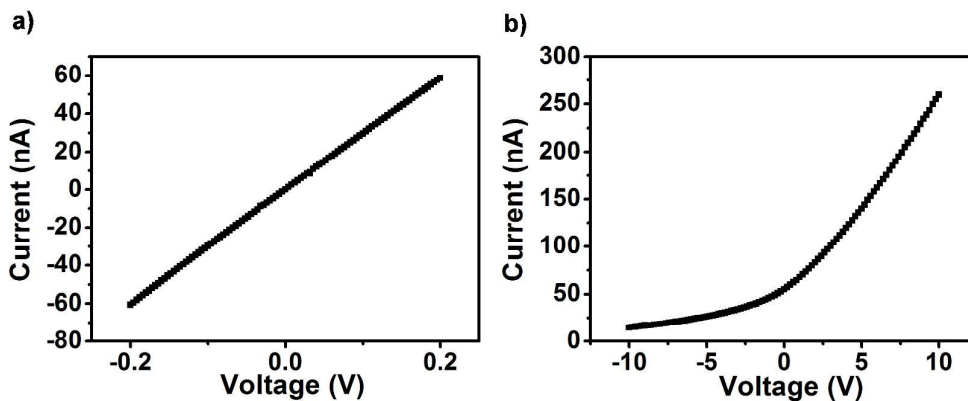


Figure S1. a) I-V characteristic between source and drain of a representative ZnO nanowire FET device measured in two-point configuration. b) Current versus back-gate voltage measured in a representative ZnO nanowire FET device.

Three terminal I-V characteristics of ZnO nanowire field-effect transistor (FET) were measured with a parameter analyzer (E5270B) by direct probing using a Wentworth micromanipulator 6200 probe station. The measurements were carried out at room temperature in air under ambient light conditions.

Electrical characterization of the ZnO NW FET devices was performed in order to investigate the properties of ZnO nanowires. I-V characteristic showed an Ohmic behavior with device resistance in the range of $10^5 - 10^6 \Omega$ and negligible contact resistance for all measured devices. From the transconductance measurements we observed the clear n-type behavior demonstrating an unintentional doping of the ZnO nanowire due to structural defects. The electron mobility was calculated by using

$$\mu = \left. \frac{dI}{dV_g} \right|_{V_{D-S}} \cdot \frac{L^2}{C_{NW} \cdot V_{D-S}}$$

where L is the nanowire length, V_{D-S} is the source-drain voltage and capacitance C_{NW} was calculated from the analytical expression

$$C_{NW} = \frac{2\pi\epsilon\epsilon_0 L}{\ln\left(\frac{2h}{r}\right)}$$

with h the thickness of the SiO_2 and r the nanowire radius. The calculated field-effect mobility was estimated to be $40 \text{ cm}^2/\text{V s}$ in agreement with previous reports.⁴ Carrier concentration was calculated using the Drude approximation by

$$n = \frac{1}{\mu e \rho}$$

with e the elementary charge and ρ the nanowire resistivity. The carrier concentration was estimated to be 10^{17} cm^{-3} .

Finally, we show the I-V characteristic and the transfer characteristic on the same hybrid device in dark condition and under laser illumination at 650 nm in figure S2. Both the I-V curves showed no measurable photocurrent with 0 V_{SD} applied and an evident linear behavior. In b), the transfer characteristic is reported showing larger current under illumination accordingly to the expected increasing of free charges due to the hot-electron mechanism (and partially due to the excitation of defect states in the ZnO nanowire).

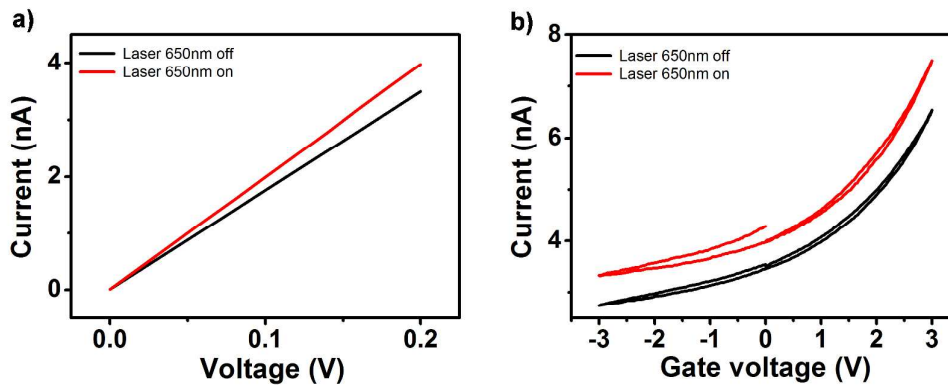


Figure S2. Comparison between the electrical response of representative hybrid FET device in dark condition (black curve) and under illumination with a laser at 650 nm (red curve) in a) I-V characteristic and b) transfer characteristic.

UV photoresponse of ZnO nanowire and hybrid device

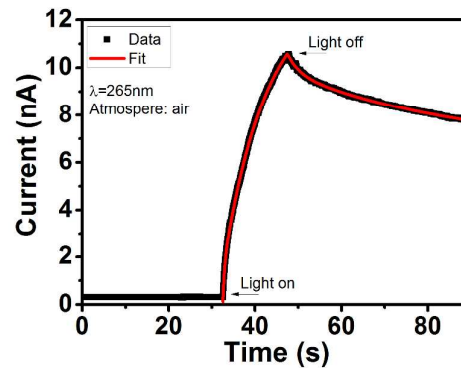


Figure S3. Photoresponse of hybrid device in air during 15s exposition to UV light (265 nm). Red lines are the bi-exponential growth and decay fitting to the corresponding data.

Figure S2 shows the photoresponse of hybrid device in air during 15s exposition to UV light (265 nm). The experimental data were well reproduced by the eq.1-2 and the following values for the parameters were obtained: $A_0 = 0.82 \pm 0.2$ nA , $A_1 = 12.41 \pm 0.02$ nA , $A_2 = 5.85 \pm 2$ nA , $\tau_1 = 10.01 \pm 0.07$ s and $\tau_2 = 0.39 \pm 0.02$ s and $B_0 = 6.53 \pm 0.03$ nA, $B_1 = 0.948 \pm 0.007$ nA, $B_2 = 3.29 \pm 0.02$ nA, $\gamma_1 = 2.74 \pm 0.05$ s and $\gamma_2 = 43.3 \pm 0.7$ s.

Photoresponse of a bare ZnO nanowire in air during 200s exposition to UV light (265 nm) is reported in Figure S3. From the bi-exponential fit were obtained: $A_0 = 209 \pm 1$ nA , $A_1 = 306 \pm 1$ nA , $A_2 = 200 \pm 1$ nA , $\tau_1 = 118 \pm 2$ s and $\tau_2 = 9.7 \pm 0.1$ s and for the photocurrent decay where the values $B_0 = 33.4 \pm 0.2$ nA, $B_1 = 297.7 \pm 0.4$ nA, $B_2 = 124.8 \pm 0.5$ nA, $\gamma_1 = 371 \pm 1$ s and $\gamma_2 = 50.1 \pm 0.3$ s. Notably, under high vacuum condition (Figure S4) the time constants increased considerably. From the data fit we obtained $A_0 = 58 \pm 1$ nA, $A_1 = 0.7 \pm 0.2$ μ A, $A_2 = 56 \pm 1$ nA, $\tau_1 = 2432 \pm 964$ s and $\tau_2 = 39.7 \pm 0.7$ s and for the photocurrent decay $B_0 = 16.7 \pm 0.5$ nA, $B_1 = 18.5 \pm 0.8$ nA, $B_2 = 330 \pm 29$ nA, $\gamma_1 = 3908 \pm$ s and $\gamma_2 = 101154 \pm 164$ s.

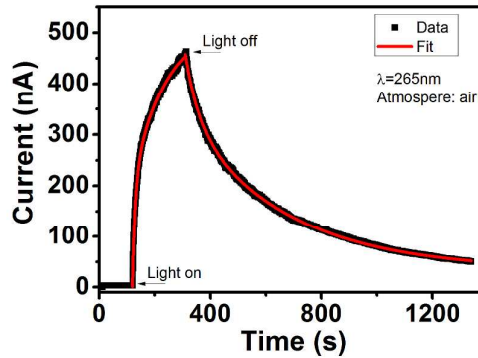


Figure S4. Photoresponse of ZnO nanowire in air device during 200s exposition to UV light (265 nm). Red lines are the bi-exponential growth and decay fitting to the corresponding data.

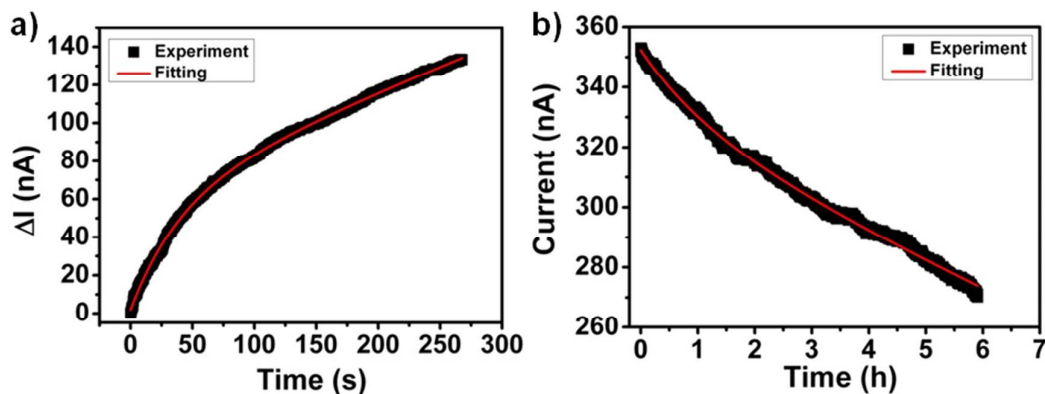


Figure S5. Photoresponse of ZnO nanowire in vacuum device during 300s exposition to UV light (265 nm). Red lines are the bi-exponential growth and decay fitting to the corresponding data.

Depolarizing factor of a prolate ellipsoid

The depolarizing factor along the main axis L_a for a prolate ellipsoid can be simplified as⁵

$$L_a = \frac{b^2}{2a^2e^2} \left[\ln\left(\frac{1+e}{1-e}\right) - 2e \right] \quad (s1)$$

where $e = \sqrt{1 - b^2/a^2}$ is the eccentricity of the ellipsoid and a and b the semiaxes of the ellipsoid.

The average geometrical depolarizing factor L_{am} obtained from the statistical length (54nm) and diameter (22nm) of the nanorods was 0.13 ± 0.03

REFERENCES

1. Borchers, C.; Müller, S.; Stichtenoth, D.; Schwen, D.; Ronning, C., Catalyst–Nanostructure Interaction in the Growth of 1-D ZnO Nanostructures. *J. Phys. Chem. B* **2006**, *110* (4), 1656-1660.
2. Nikoobakht, B.; El-Sayed, M. A., Preparation and Growth Mechanism of Gold Nanorods (NRs) Using Seed-Mediated Growth Method. *Chem. Mater.* **2003**, *15* (10), 1957-1962.
3. Nikoobakht, B.; El-Sayed, M. A., Evidence for Bilayer Assembly of Cationic Surfactants on the Surface of Gold Nanorods. *Langmuir* **2001**, *17* (20), 6368-6374.
4. Goldberger, J.; Sirbully, D. J.; Law, M.; Yang, P., ZnO Nanowire Transistors. *J. Phys. Chem. B* **2004**, *109* (1), 9-14.

5. Jones, T. B., *Electromechanics of particles*. Cambridge Univ Pr: 2005.